

Enhanced maximum power tracking for PV energy system using new optimized P&O algorithm with cyclic measurement tracking controller

R.Arulmurugan¹

¹Dept of EEE, Research Scholar, Anna University, Chennai, India
contact: ¹arul.lect@gmail.com,

Dr.N.Suthanthiravanitha²

²Prof and head, Dept of EEE, Knowledge Institute of Technology, Salem, India
contact: ²varmans03@gmail.com

Abstract :- *In furthermost of the maximum peak power point tracking approaches described presently in the literature, the finest function point of the photovoltaic schemes is assessed by linear calculations. Nevertheless these estimates can lead to less than optimum functioning conditions and henceforth decrease significantly the performances of the photovoltaic scheme. This paper presents a novel technique to determine the peak power point based on observes of the open circuit voltage of the photovoltaic cells, and a nonlinear expression for the optimum functioning voltage is established based on this open circuit voltage. The methodology is thus a mixture of the nonlinear and enhanced perturb and observe (P&O) algorithm. The simulation and experimental consequences show that the method develops clearly the tracing efficiency of the extreme power obtainable at the production of the photovoltaic array. The new technique decreases the fluctuations around the peak power point, and raises the average efficiency of the maximum power point tracking attained. The novel maximum power tracking technique will provide additional power to energy storage.*

Index Terms:- *Enhanced perturb and observe algorithm, repeated tracking reference, standalone photovoltaic, open circuit voltage.*

1. INTRODUCTION

The functioning power of PV array depends on the solar temperature, radiation and particularly the photovoltaic array output voltage [1]. If the transferal of power between photovoltaic panel and battery load is not optimum, the entire efficacy of the photovoltaic structure will be suffered harmfully [2]. Numerous publications challenge the problem regarding the search of the

optimum working point by utilizing various MPPT approaches in order to excerpt the supreme energy from the photovoltaic panel [3]. The mainstream of these initial approaches are based on so-named hill climbing method [4]. These approaches can be utilized to regulate the peak power point for identified solar temperature and radiation situations; though they exhibit oscillatory actions around the peak power point under normal working conditions. Furthermore, they can lead to a wrong path of the peak power point tracing (i.e. to smaller amount efficiency) in the case of an abrupt difference of irradiance and/or temperature when the scheme is already very close its real peak power point [5]. This is for the reason that the P&O procedure interprets the perturbation as the consequence of its previous difference of the modules working voltage, and guesses its next deviation to be in the similar path as that of the earlier one. These approaches have the famous weakness of producing improvements that, when the arrangement is already functioning at or very close its optimal power point, take it away from that location when a variation in ambient situations adjust the production power of the photovoltaic array [6]. The next MPPT technique, based on look-up tables of the PV array characteristics, ought to be talented to promptly regulate the best point of process when temperature and/or irradiation values are accessible; nevertheless the nonlinearity and the deviation of the characteristics of the PV modules as a function of these variables make the establishing and the storing of a consistent look-up table somewhat problematic [7]. The third MPPT techniques, based on the calculated modelling of the nonlinear voltage versus current characteristics of the photovoltaic array, can be modest and talented to rapidly determine the

best process point of the photovoltaic scheme [8]. When utilizing this modelling of the voltage versus current characteristics process, the maximum power point is approached for numerous situations of load by a linear role of the open circuit voltage or of the short circuit current [9]. Though that technique has its peculiar problems, as the proportion between open circuit voltage and optimal operating voltage differs rendering to varying situations of temperature and irradiation, and also that it is incredible to regulate the open circuit voltage by utilizing only single linear function of the voltage [10].

This paper progresses a nonlinear peak power point tracking method based on observes of the open circuit voltage in instruction to read optimum working conditions for the photovoltaic array. The mixture of this method with enhanced Perturb and Observe algorithm technique greatly advances the performance of the peak power point tracing of the photovoltaic schemes. This new enhanced maximum power point tracing technique is appropriate to any kind of load attached to the photovoltaic modules.

NOMENCLATURE

PV	Photovoltaic
q	Electron Charge
K_b	Boltzmann's Constant
T_c	Cell's Working Temperature
A	Ideal Factor
R_{SH}	Shunt Resistance
R_{SE}	Series Resistance
I_{SC}	Cell's Short Circuit Current
I_{RS}	Cells Reverse Saturation Current
I_{PV}	Light Generated Current or Photocurrent
I_o	Cell Saturation of Dark Current
G	Irradiance
T	Temperature
V_{OC}	Open circuit voltage
N_s	Series number of cells for a PV module
N_p	Parallel number of cells for a PV module
I_{ph}	Cell light generated current
I_{OS}	Reverse saturation current
R_{OP}	optimum load

n	Ideality factor
R_{load}	Load resistance
I_{sc}^*	PV array short circuit current at the reference
P_{OP}	optimum power
V_{oc}^*	PV array open circuit voltage at the reference
G^*	Reference solar irradiance
T^*	Reference solar temperature
α_1, α_2	Cell Temperature coefficients for current and voltage
R_{on}	International resistance
PWM	Pulse Width Modulation
SW	Switch
I_{PV}, V_{PV}	Output current; output voltage

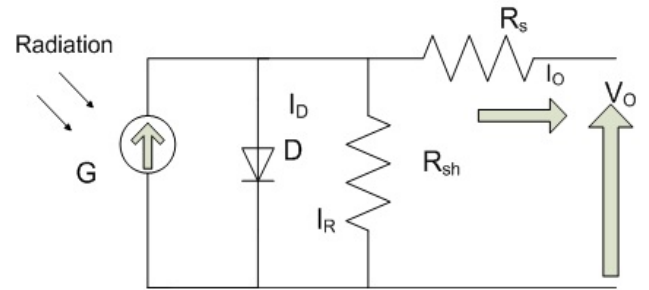


Fig.1 Equivalent circuit model of PV panel

2. PV MODULE CHARACTERISTICS

The corresponding electric figure of a photovoltaic array is revealed in Fig.1. The photovoltaic array electric characteristics under sun irradiance are specified in expressions of I_{PV} and V_{PV} [11].

$$I_{PV} = I_L - I_o \left[e^{\left(\frac{V_{PV} + R_{SE} I_{PV}}{V_T} \right)} - 1 \right] - \frac{V_{PV} + R_{SE} I_{PV}}{R_{SH}} \quad (1)$$

Where $I_L = N_p I_{ph}$ related to the light produced current of the PV panel. $I_o = N_p I_{OS}$ relates to the reverse saturation current of the PV panel. $V_T = (N_s n K_B T) / q$ denoted as the thermal voltage,

The PV array: I_{SC} and V_{OC} at solar radiation G and temperature T are specified by

$$I_{SC} = I_{SC}^* \left(\frac{G}{G^*} \right) + \alpha_1 (T - T^*) \quad (2)$$

$$V_{OC} = V_{OC}^* + \alpha_2 (T - T^*) - (I_{SC} * I_{SC}^*) R_{SE} \quad (3)$$

An ideal PV module is one for which R_{SC} is zero and R_{SH} is infinitely large. The output I_{PV} and V_{PV} are

$$I_{PV} = I_L - I_o \left[e^{\left(\frac{V_{PV}}{V_T} \right)} - 1 \right] \quad (4)$$

$$V_{PV} = V_T \ln \left[\frac{I_L - I_{PV}}{I_o} + 1 \right] \quad (5)$$

Generally photovoltaic modules characteristic offerings three significant points: I_{SC} , V_{OC} and P_{OP} delivered by the photovoltaic modules to R_{OP} when the photovoltaic array functions at their maximum power point.

3. SYSTEM DESCRIPTION

Fig.2 shows the block diagram of proposed novel converter controller. It includes 40 Wp PV array, DC to DC buck-boost zeta converter, battery load and new enhanced Perturb and Observe method with repeated observation tracing reference controller. The DC to DC converter is collected of a control and power part. The switch SW of the DC to DC buck-boost converter is a Mosfet with a short R_{on} . The power switches of MOSFET are controlled by a Pulse Width Modulation signal production circuit that uses a microcontroller. T represents the time period of the control signal and D denotes the duty cycle. The SW is locked for the dT Time period and unlocked for $(1-d)T$ time period [15]. In finding for the maximum power point and tracing this point in order to reduce the spread between the optimal power in the event of alteration of the climate conditions and working power, the controller circuit of the DC to DC buck-boost zeta converter insincerely perturbs occasionally the functioning point of the photovoltaic module. The resultant output current and voltage of the photovoltaic modules are then utilized by the controller circuit to rise or drop the D of the buck-boost converter in order to variation the functioning point of the photovoltaic array. If the P (power) is thereby raised, then the subsequent perturbation will be in the similar direction; else the subsequent perturbation will be in the conflicting direction.

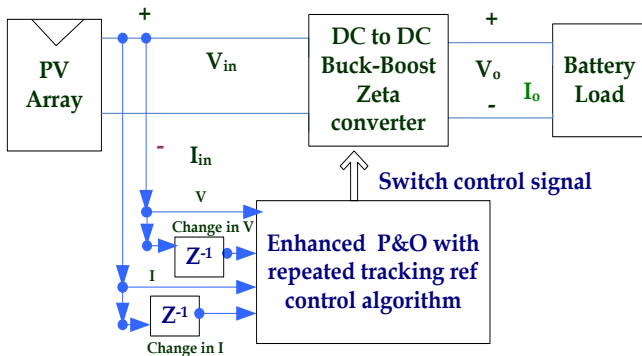


Fig.2 Block diagram representation of proposed scheme

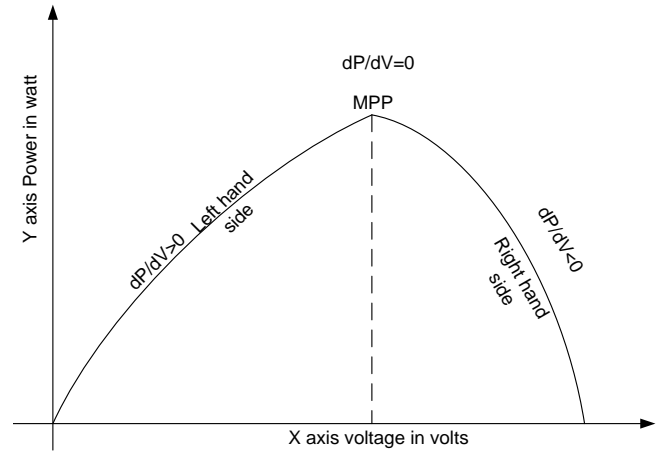


Fig.3 Conceivable movements of the working point.

4. NOVEL ENHANCED PERTURB AND OBSERVE TRACKING ANALYSIS

The adjustable load obligatory generating maximum power as a function of changing conditions of temperature and irradiance will be the input resistance of the converter. When the solar temperature and radiation differed as exposed in Figs.8-9, each of the maximum power points relates to only single value of the input resistance of the converter. Then when the solar temperature or radiation variations, the value of input resistance seen by PV array must be altered to locate the new maximum power point and this will be attained by changing the duty cycle. In past decades, the maximum power point tracking approaches produced resulted in fluctuations of the spot of the maximum power point which can really lead it away from its best value. In direction to overcome this problem, an investigation is provided to recognise the expected movement of the functioning point resulting from a functional perturbation of the working conditions [12]. Fig.3 shows the classic graph of photovoltaic power difference according to the functioning voltage. This graph demonstrates that there are two functioning regions: the first is located on the right hand side of the maximum power point where $\Delta P/\Delta V < 0$ and another on the left hand side of the peak power point where $\Delta P/\Delta V > 0$.

Six suitcases of perturbations from the functioning point can be distinguished: First case: After the perturbation, there is a movement of the functioning point from $z-1$ to z , with $P(z) > P(z-1)$ and $V(z) < V(z-1)$. The power rises after the perturbation. This specifies that the maximum power point search is oriented in the correct

way. The find of the maximum power point continues in the same way and grasps the functioning point $z+1$ by increasing the duty cycle by ΔD . The voltage is then improved to $D=D+\Delta D$. Second case: After the perturbation, there is a movement of the working point from $z-1$ to z , with $P(z)<P(z-1)$ and $V(z)>V(z-1)$. The power decreases after the perturbation. This specifies that the maximum power point search is oriented in the wrong way. The maximum power point search way must be changed and the duty cycle is increased by ΔD to reach the working point $z+1$. The voltage is then raised to $D=D+\Delta D$. Third case: After the perturbation, there is a displacement of the operating point from $z-1$ to z so that $P(z)>P(z-1)$, $V(z)>V(z-1)$ and $I(z)>I(z-1)$. The power rises after perturbation. This specifies that the maximum power point search is oriented to the good direction. Then, the maximum power point search direction must be maintained and the duty cycle is increased by ΔD_2 to reach the functioning point $z+1$. The voltage is then increased to $D=D+\Delta D_2$. Fourth case: After the perturbation, there is a displacement of the operating point from $z-1$ to z so that $P(z)>P(z-1)$, $V(z)>V(z-1)$ and $I(z)<I(z-1)$. The power rises after perturbation. This specifies that the maximum power point search is oriented to the good direction. Then, the maximum power point search direction must be maintained and the duty cycle is reduced by $-\Delta D$ to reach the functioning point $z+1$. The voltage is then decreased to $D=D-\Delta D$. Fifth case: After the perturbation, there is a displacement of the operating point from $z-1$ to z so that $P(z)<P(z-1)$, $V(z)<V(z-1)$ and $I(z)<I(z-1)$. The power decreases after perturbation. This specifies that the maximum power point search is oriented to the bad direction. Then, the maximum power point search direction must be maintained and the duty cycle is reduced by $-\Delta D_1$ to reach the functioning point $z+1$. The voltage is then decreased to $D=D-\Delta D_1$. Sixth case: After the perturbation, there is a displacement of the operating point from $z-1$ to z so that $P(z)<P(z-1)$, $V(z)<V(z-1)$ and $I(z)>I(z-1)$. The power decreases after perturbation. This specifies that the maximum power point search is oriented to the bad direction. Then, the maximum power point search direction must be maintained and the duty cycle is

reduced by $-\Delta D$ to reach the functioning point $z+1$. The voltage is then decreased to $D=D-\Delta D$.

Table-I Summary of controller process for numerous functioning points

Case	ΔP	ΔV	ΔI	Tracing Direction	Control action of duty cycle
1	+	-		Correct way	$D=D+\Delta D$
2	-	+		Opposite way	$D=D+\Delta D$
3	+	+	+	Correct way	$D=D+\Delta D_2$
4	+	+	-	Correct way	$D=D-\Delta D$
5	-	-	-	Opposite way	$D=D-\Delta D_1$
6	-	-	+	Opposite way	$D=D-\Delta D$

The find the rules for the six cases of process are summarized in Table-I. Obviously cases 1, 3 and 4 continue in the correct way, whereas cases 2,5 and 6 must opposite way.

5. NEW ENHANCED P&O BASED REPEATED OBSERVATION TRACING REFERENCE OF MPPT CONTROLLER

5.1. Output voltage and output current based maximum power point tracking

To evaluate the optimal working point corresponding to the supreme power for the numerous levels of sun irradiance, temperature, mathematical approaches can be utilized to demonstration the linear dependence between the open circuit voltage and optimal voltage [11]. The simple general equation can be written as

$$V_{OP} = K_v V_{OC} \quad (6)$$

Where K_v is the proportionality constant of voltage.

This mathematical approach the key idea of the method called voltage based maximum power tracking. A same tactic, based on the linear calculation of the optimal current relative to the short circuit current, can also be utilized to find out the maximum power point. The following equation characterizes this concept of method called current based maximum power tracking.

$$I_{OP} = K_i I_{SC} \quad (7)$$

Where K_i is the proportionality constant of current.

The voltage and current based maximum tracking approaches may be utilized either with boost converter or buck converter, contingent on the load characteristics. I_{sc} depends linearly on the sun irradiance, while the V_{oc} depends logarithmically on the sun irradiation. The literature survey tends to demonstration that the linear estimate of the current based maximum power tracking method is higher accurate when matched with the linear approximation of the voltage based maximum power tracking method. Nevertheless, the method of voltage based maximum tracking is loss less and more effective. Moreover, real time observation of photovoltaic I_{sc} and I_o make current based maximum power tracking hardware greater complex associated with voltage based maximum power tracking circuitry. From this investigation, a new nonlinear tactic of the maximum power point value assessment is proposed.

5.2. New enhanced P&O with repeated observation approach

The methodology is based on the V_{oc} observe and a nonlinear design of the optimal voltage. Supreme power is attained by cancelling the derivative of the power.

$$P_{OP} = V_{OP} \times I_{OP} \quad (8)$$

$$\frac{dP}{dI_{PV}} = \frac{d(I_{PV} V_{PV})}{dI_{PV}} = 0 \quad (9)$$

This leads to

$$\left(\frac{dV_{PV}}{dI_{PV}}\right)_{OP} = -\frac{V_{OP}}{I_{OP}} \quad (10)$$

$$V_{PV} = V_T \ln\left[\frac{I_L - I_{PV}}{I_o} + 1\right] \quad (11)$$

$$\frac{V_{OP}}{I_{OP}} = \ln\left[\frac{(I_L - I_{PV})}{(I_o)} + 1\right] \quad (12)$$

$$dV_{PV} = V_T \times \frac{1}{\left[\frac{I_L - I_{PV}}{I_o} + 1\right]} \quad (13)$$

$$dV_{PV} = V_T \times \frac{I_o}{[I_L - I_{PV} + I_o]} \quad (14)$$

$$I_L = I_{sc} \quad (15)$$

The derivative of the relation of above equation is put into Eq.(10) stretches

$$\frac{V_{OP}}{I_{OP}} = -\frac{V_T}{(I_o + I_{sc} - I_{OP})} \quad (16)$$

Taking into account Eq.(7), V_{OP} can be found as

$$V_{OP} = \frac{I_{OP} V_T}{\left(1 - \frac{1}{K_i}\right) I_{OP} - I_o} \quad (17)$$

The V_{oc} of the photovoltaic array is written by

$$V_{oc} = V_T \ln\left[\frac{I_{sc}}{I_o} + 1\right] \quad (18)$$

The Optimal current is presumed from Eq.(10) and Eq.(17).

$$I_{OP} = K I_o \left[e^{\left(\frac{V_{oc}}{V_T}\right)} - 1 \right] \quad (19)$$

The optimal voltage can be calculated from Eq.(10) and Eq.(19).

$$V_{OP} = \frac{V_T \left[e^{\left(\frac{V_{oc}}{V_T}\right)} - 1 \right]}{\left(1 - \frac{1}{K_i}\right) e^{\left(\frac{V_{oc}}{V_T}\right)} - 1} \quad (20)$$

Fig.4 gives the flow chart algorithm of the new technique based on this nonlinear tactic. To evaluation the maximum power point reference value, the V_{oc} of the photovoltaic panel is observed regularly at the output PV array during the turn-off (opening) of the SW of the buck-boost zeta converter. The measured voltage permits the maximum power point reference value to be designed from Eq.(20), and subsequently the value of the DC to DC buck-boost converter “D” to be attuned.

The output power of a PV cell is getting changed with a fluctuating irradiation and temperature. Consequently a MPP technique is used to obtain peak power from a photovoltaic array under changing functioning point have been suggested. The nonlinear maximum power point tracking method based on the observes of the open circuit voltage in order to read best function conditions for the photovoltaic panel. The arrangement of the this open circuit voltage method with the new enhanced Perturb and Observe technique largely advances the performance of the maximum power point tracking of the photovoltaic scheme. This novel maximum tracking approach is appropriate to any kind of load coupled to the photovoltaic panel. The enhanced algorithm is capable of tracking the maximum power under the rapid changes in atmospheric conditions with high accuracy compared to existing system. The enhanced P&O algorithm description is as follows [12].

The enhanced P&O method overcomes the problem of conventional perturb and observe method such as failing to track the maximum power under various atmospheric condition. The proposed system uses the current versus voltage curve method to avoid the happening as in conventional P&O method. In fixed G condition, when the current rises (reductions), the voltage reduces (rises).

Using this easy statistic, can be answered the problems of conventional P and O from the real MPP in quickly varying environmental circumstances, as follow. If the power and the current instantaneously rise and then voltage rises too, the algorithm recognizes that it is in quickly varying environmental circumstances and reductions the current, instead, it rises. When the power and the current are rising instantaneously and the voltage is reducing, algorithm is in fixed illumination and raises the current. Hence the maximum power point tracking technique avoids conflicting from the real maximum power point. The enhanced perturbation and observation technique are obtained in Fig.4.

Fig.4. Enhanced P and O algorithm with repeated measurement tracing reference

5.3 DC to DC Buck-Boost Zeta Conversion and Control Scheme

According to the maximum power transfer theory, maximum power achieved means that the photovoltaic generating system is always supposed to operate at maximum output voltage [13], [14]. Usually, an appropriate controller is a DC to DC converter, which is widely used in PV power systems as a matching interface between the PV panel and the load. Hence the main function of a these controller is to adjust the panel output voltage to a value in which the panel transfers maximum energy to the load by controlling the on-off times of the converter's power switch. The power delivered to the load is a maximum when the source internal impedance matches the load impedance.

A DC to DC converter with maximum power point controller offers high efficiency over a wide range of operating points. The full power may not be delivered to the load completely due to the power loss for a without converter. Therefore, the design of a good performance converter is a very important issue. The block diagram of the DC to DC converter controller proposed in this work is shown in Fig.2. A DC to DC converter is used to interface the PV output to the load and to track the maximum power of the PV modules. A more detailed schematic is illustrated in Fig.5. Usually, Topologies of DC to DC converters [15] have mainly buck, boost, buck-boost and Cuk, etc. In this study we chose the buck-boost zeta converter circuit.

The ZETA DC to DC converter is similar to the buck-boost topology varies the above and below the output voltage. This converter needs two inductors and one series capacitor, sometime this capacitor is called a flying capacitor. The zeta converter basically is configured from a buck controller that drives a high side PMOSFET. The zeta converter is one more option for regulating a nonlinear input power supply, like low cost wall wart. In the design of the converter to minimize board space, a coupled inductor can be used.

5.3.1 Modes operation of zeta converter

The illumination of Fig.5 shows a simple circuit of a ZETA converter, containing of an input capacitor, C_{in} , an output capacitor, C_{out} , coupled inductors L_1 and L_2 , an AC

coupling capacitor C, a power MOSFET, SW_1 , and a diode, D.

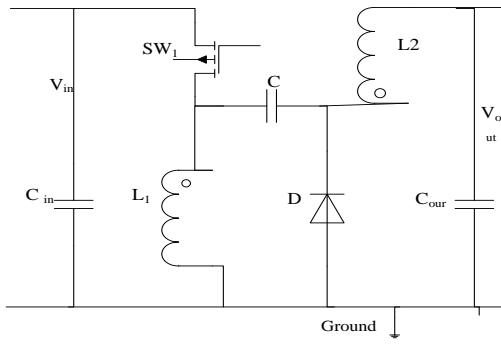


Fig.5. DC to DC buck-boost zeta converter

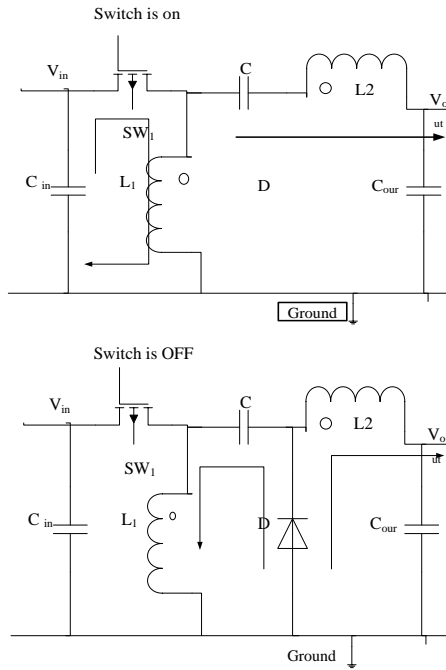


Fig.6. Converter circuit diagram (a) switch is on (b) switch is off

Fig.6 shows the ZETA converter operating in the continuous conduction mode (CCM) when SW_1 is on and when SW_1 is off. To recognize the voltages at the various circuit nodes, it is essential to analyse the circuit at DC when both switches are off and not switching. Capacitor (C) will be in parallel with C_{out} , so C is charged to the output voltage, V_{out} , during steady state CCM. Fig.6. illustrates the voltages across L_1 and L_2 during CCM operation. When SW_1 is off, the voltage across L_2 must be V_{out} since it is in parallel with C_{out} . Since C_{out} is charged to V_{out} , the voltage across SW_1 when SW_1 is off is $V_{in} + V_{out}$, therefore the voltage across L_1 is $-V_{out}$ relative to the drain of SW_1 . When SW_1 is on, capacitor C, charged to V_{out} , is connected in series with L_2 , so the voltage across L_2 is $+V_{in}$, and diode D sees $V_{in} + V_{out}$ [16]. When

SW_1 is on, energy from the input supply is being stored in L_1 , L_2 , and C. L_2 also provides I_{out} . When SW_1 turns off, L_1 's current continues to flow from current provided by C, and L_2 again provides I_{out} . The duty cycle D for a zeta converter operating in CCM is given by

$$D = \frac{V_{out}}{V_{in} + V_{out}} \quad (21)$$

This can be rewrite as

$$\frac{D}{1-D} = \frac{I_{in}}{I_{out}} = \frac{V_{out}}{V_{in}} \quad (22)$$

D_{max} occurs at $V_{in(min)}$ and D_{min} occurs at $V_{in(max)}$.

6. RESULTS

The simulation and experimental investigations were passed out on the test bench of the portable standalone photovoltaic renewable energy scheme installed at the Government College of Engineering, Salem, Tamil Nadu, and India [17]. The test sets contains a 40 W_p photovoltaic panel consists of four modules each 10 W_p respectively sponsored by IIT-Bombay, DC to DC buck-boost zeta converter, new enhanced P&O with repeated tracing reference controller and battery load. The photovoltaic array has been utilized for charging the battery load, which will operate as buffer drive storage for the scheme. The simulation model of schematic diagram is revealed in Fig.7. The designed new algorithm and the conventional Perturb and Observe approaches were matched by simulations tools using Matlab/Simulink software. Fig.8 and Fig.9 stretch the Voltage versus Current (V vs. I); Voltage versus Power (V vs. P) characteristics of a photovoltaic array for altered values of solar temperature and irradiation. The I_{sc} is clearly proportional to the sun radiation (Fig.8): Higher radiation, additional current and more supreme power output. On another side the temperature dependence is opposite (Fig.8): a rise in 'T' causes a reduction of the V_{oc} (when adequately great) and henceforth also of the supreme power output. Therefore these conflicting effects of the deviations of solar temperature and irradiance on the supreme power output create it significant to trace the maximum power point efficiently. The voltage versus power curves of Figs.8&9 demonstrations that the best power point relates to a load joined to the photovoltaic array that fluctuates with the ambient situations of T & G.

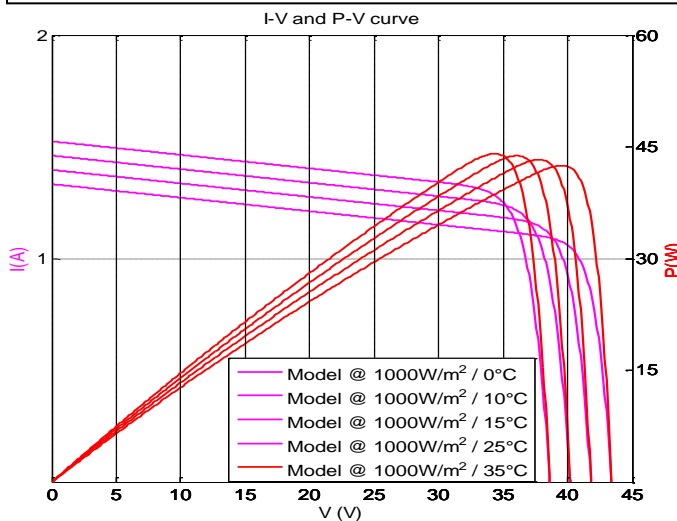
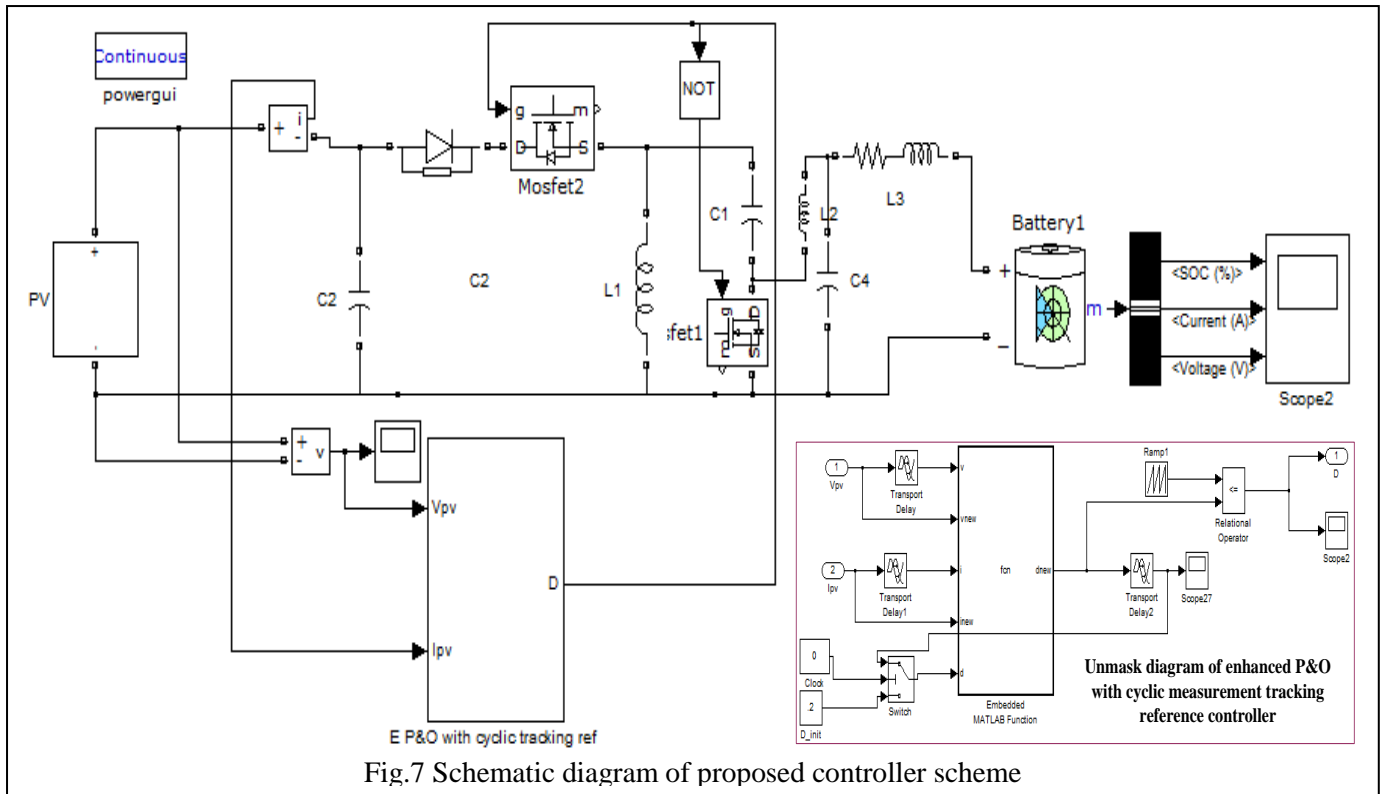


Fig.8 V-I and V-P characteristics curves of change in solar irradiance influence

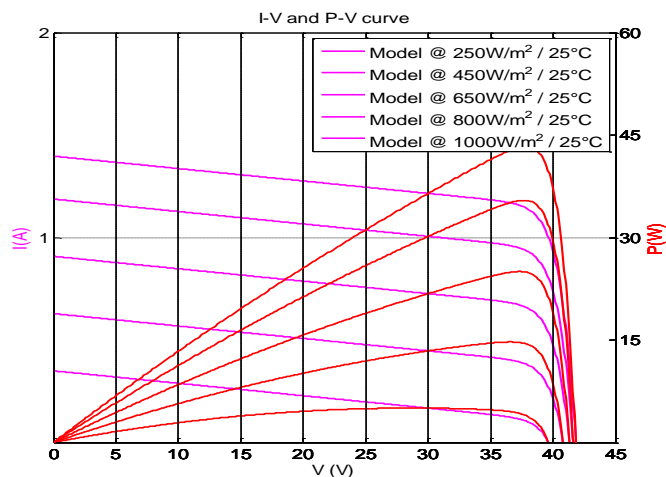


Fig.9 V-I and V-P characteristics curves of change in solar temperature influence

In exercise this adjustable best load will be attained through the use of an adjustable 'D' of the controller part of the maximum power point tracking DC to DC converter, which controls straight the functioning voltage which relates to this best load. The simulation consequences are exposed in Figs.8&9. The sun radiation sketch is supposed to be rising linearly. With the designed new maximum power tracking technique (Figs.8-9), the fluctuations about the maximum power point are totally eradicated [18].

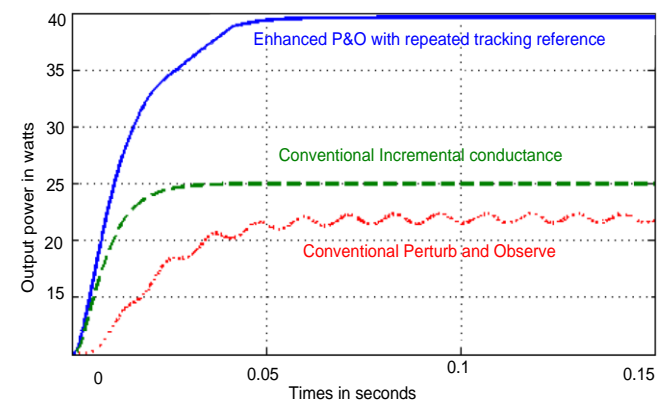


Fig.10 Output power of the PV array using the novel enhanced P&O with repeated tracking reference and the conventional technique.

Fig.10 demonstrations the available output power of the photovoltaic array when using the designed technique and the conventional technique. The supreme power and sun radiation are considered from the characteristics of the

constructed PV array sponsored by IIT, Bombay. To authenticate the designed new maximum power point tracking algorithm, a comparison is completed between the conventional P&O algorithm and the above new enhanced P&O with repeated observation method [19]. The evaluation was based on the output power of the supreme power obtainable at the PV panels. The MPPT tracing efficiency is distinct as [2]

$$\eta_T = \frac{1}{n} \sum_{i=1}^n \frac{\text{PV module output power}}{\text{maximum power of PV modules in } n \text{ samples}} \quad (23)$$

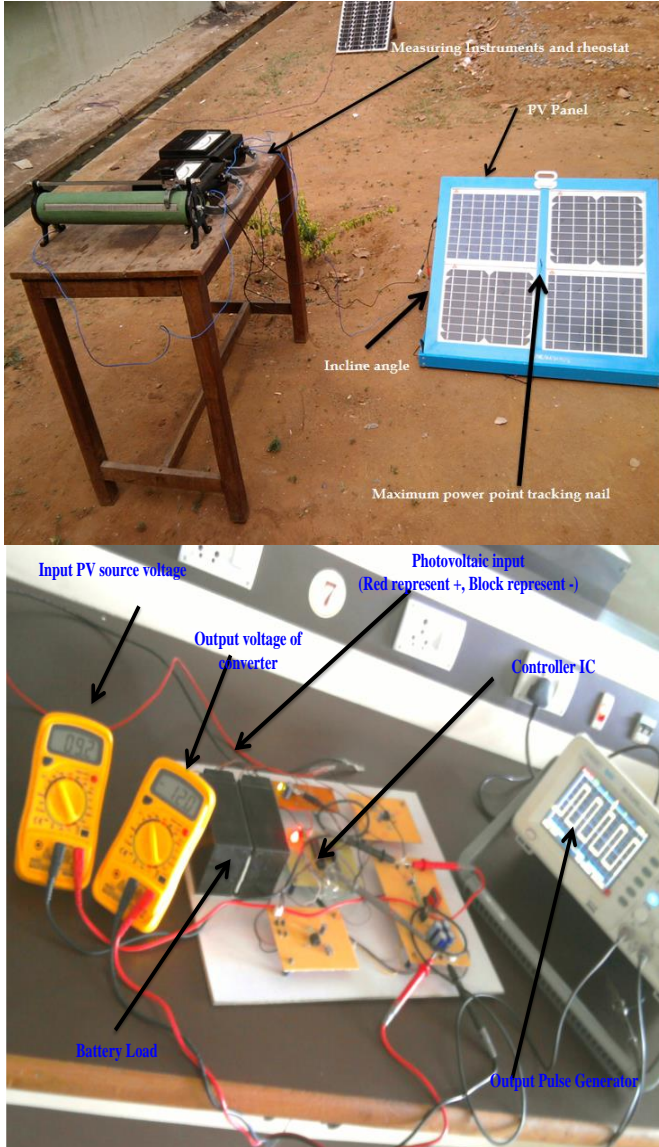


Fig.11 Photos of prototype setup (a) PV array (b) DC to DC buck-boost zeta converter with enhanced P&O repeated tracking MPPT algorithm.

6.1 Experimental Setup and Results

The process of enhanced P&O with repeated tracking reference MPP tracking algorithm has been assessed by experiment. The experimental test was carried out on the laboratory test bench of the standalone PV system

installed on the floor of the Electrical and Electronics Engineering at Government College of Engineering, Salem, India, sponsored by IIT, Bombay. A model of the suggested scheme depicted in Fig.11 composed of (a) photovoltaic panel (b) DC to DC buck-boost zeta converter with suggested controlling technique. In the test, there are four PV modules mounted side by side and is connected in series and parallel manner. AtMega 8 microcontroller was used to deliver the control pulses for the DC to DC zeta converter. The C language code of the enhanced P&O with repeated tracking reference controller and PWM generator system is constructed and debugged, and executed with the assistance of the Arr studio development tool and Proisp software [16, 17]. Fig.11 (a) displays a setup of solar PV panels connected in parallel and series arrangements. The panel is tilting stand preparation is used. Microcontroller Atmega8 was utilized to track the real PV characteristics. From the experimental results conclude that the solar illumination has been observed as proportional to short circuit current. Fig.12. shows the gate pulses generated by Atmega microcontroller with weather conditions are introduced.

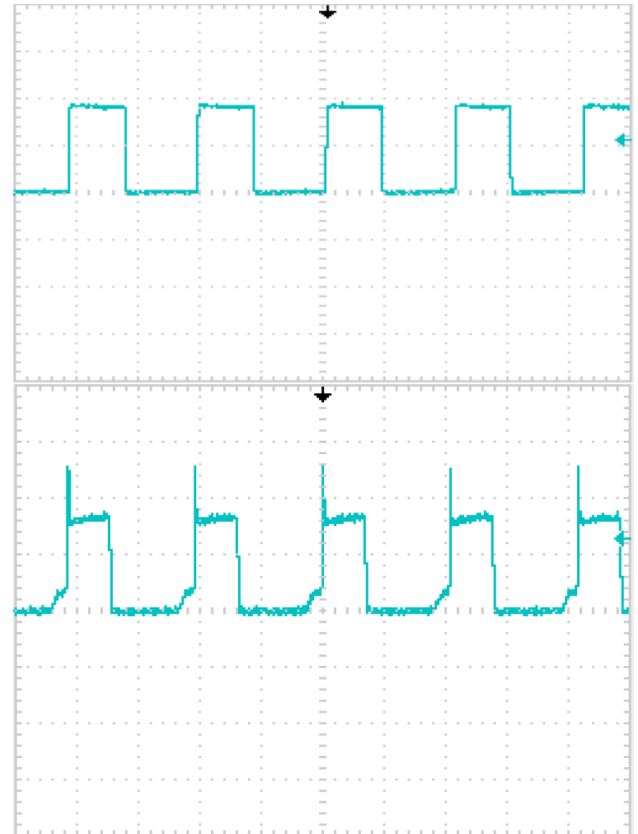


Fig.12. Experimental waveform of gate pulse and drain to source voltage of MOSFET.

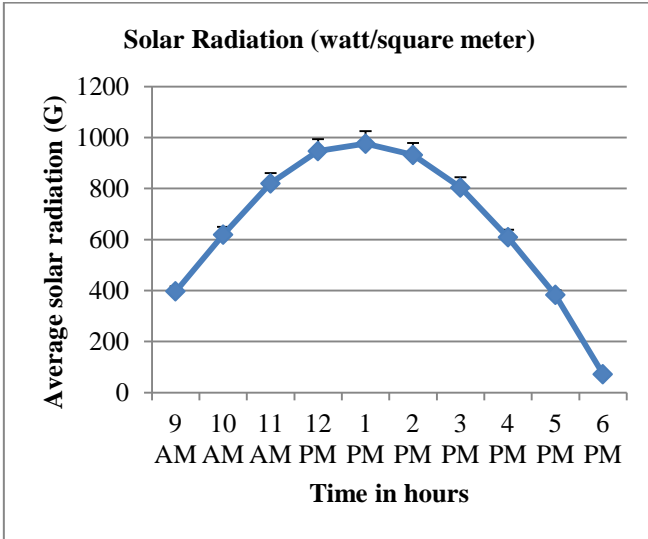


Fig.13 Solar radiation intensity for a sample day (12th March 2012 at Salem) in the form of Gaussian function.

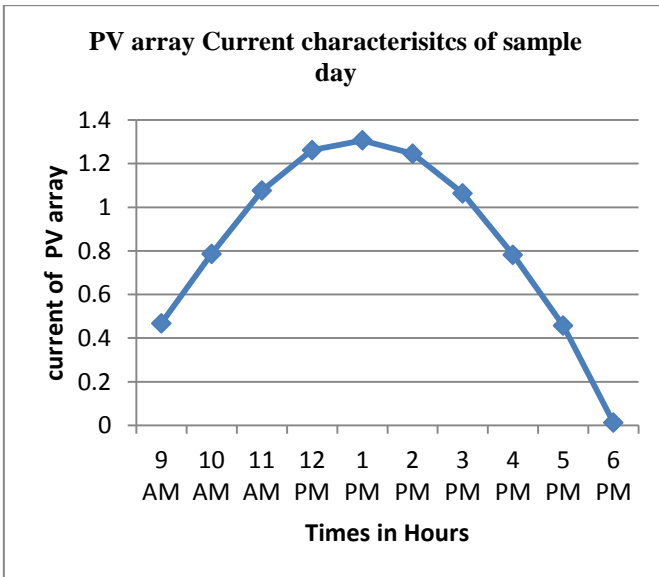


Fig.14 Current characteristics during a sample day for different voltage.

6.2 Numerical Simulation

For easiest Simulink, the sun irradiation strength for a typical day is expected to be a process of Gaussian function which is demarcated as

$$G(t) = G_{\max} \exp[-(t - t_c)^2 / 2\sigma^2] \quad (24)$$

Where G_{\max} is the greatest irradiation strength at a specified time, σ is the standard deviation of Gaussian function; t_c is the centre time, Fig.13 demonstrations a graph of the Gaussian function for the sun irradiation strength for a typical day (12th March 2012 at Salem) with the circumstances. $G_{\max}=1 \text{ KW/m}^2$, $\sigma=0.5$ and $t_c=12$. The highest of sunlight irradiance intensity happens at after noon. The module/cell temperature for a typical day is supposed to be at a stable temperature of nominal

operating cell temperature by ignoring the effect of the sun irradiation. Given sunlight radiance for a typical day, the output current is administrated by its output voltage which is determined by the ensuing load [20]. Without taking cell temperature differences into consideration, the supreme power is determined by both irradiation strength and output voltage. For different output current, voltage, and power are exposed in Figs. 14, 15 and 16 for a typical day (12th March 2012 at Salem).

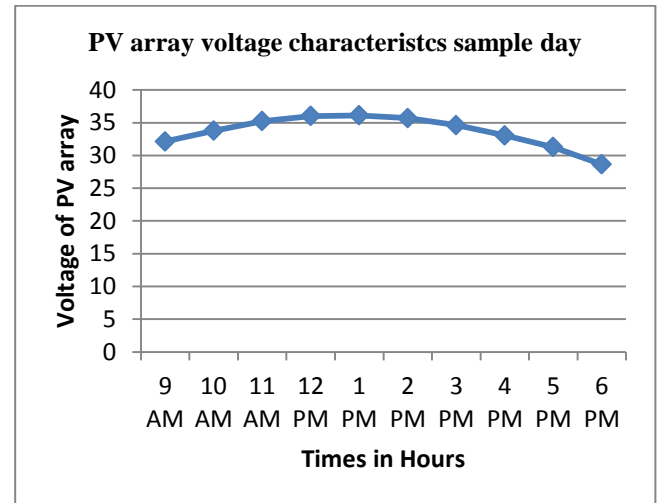


Fig.15 Voltage characteristics during a sample day (12th March 2012 at Salem) for different voltage.

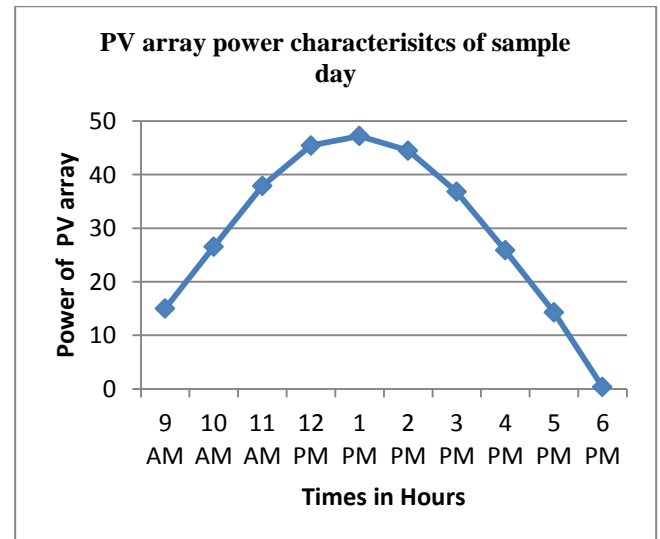


Fig.16 Power characteristics during a sample day (12th March 2012 at Salem) for different voltage.

7. CONCLUSION

A new enhanced P&O with repeated measurement tracing reference technique based on a nonlinear approach for approximating the best functioning point was established. Utilizing this technique, it is conceivable to adapt the

battery load to the photovoltaic array and to follow the maximum power point howsoever the climate situations may differ. Simulation and experimental outcomes of this new enhanced approach exhibited that the tracing efficiency of the maximum power point is improved than that gotten with the conventional Perturb and Observe technique. The new enhanced nonlinear process produced virtually no fluctuations around the maximum power point, the main drawbacks of the conventional Perturb and Observe technique. Implementation of such a technique in photovoltaic schemes will raise the power delivered to energy storage media. The simulation and experimental results show that the gain in power attained by this new enhanced technique can clearly raise the production and storage rates from photovoltaic schemes because of the enriched control of the maximum power point during varying ambient climate conditions.

References

- [1] T. Tafticht, K. Agbossou, M.L. Doumbia, A. Cheriti, "An improved maximum power point tracking method for photovoltaic systems", *Renewable Energy* 33, pp.1508–1516, 2008
- [2] D. P. Hohm and M. E. Ropp, "Comparative Study of Maximum Power Point Tracking Algorithms", *Progress in Photovoltaics: Research and applications*, 11 , pp. 47–62, 2003 (DOI: 10.1002/pip.459)
- [3] Chia-Hung Lia, Cong-Hui Huang, Yi-Chun Du, Jian-Liung Chen, "Maximum photovoltaic power tracking for the PV array using the fractional order incremental conductance method", *Applied Energy* 88, pp 4840-4847, 2011
- [4] Ahmad Al Nabulsi and Rached Dhaouadi, "Efficiency Optimization of a DSP-Based Standalone PV System Using Fuzzy Logic and Dual-MPPT Control", *IEEE Transactions on Industrial informatics*, vol. 8, no. 3, pp.573-584, august 2012
- [5] Subiyanto Subiyanto, Azah Mohamed, M.A. Hannan, "Intelligent maximum power point tracking for PV system using Hopfield neural network optimized fuzzy logic controller", *Energy and Buildings* 51, pp.29–38, 2012
- [6] Nopporn Patcharaprakiti, Suttichai Premrudeepreechacharn, Yosana Sriuthaisiriwong, "Maximum power point tracking using adaptive fuzzy logic control for grid-connected photovoltaic system", *Renewable Energy* 30, pp.1771–1788, 2005
- [7] Ali Akbar Ghassami, Seyed Mohammad Sadeghzadeh, Asma Soleimani, "A high performance maximum power point tracker for PV systems", *Electrical Power and Energy Systems* 53, pp.237–243, 2013
- [8] Liping Guo, John Y. Hung, R.M. Nelms, "Comparative evaluation of sliding mode fuzzy controller and PID controller for a boost converter", *Electric Power Systems Research* 81, pp.99–106, 2011
- [9] D. Rekioua , A.Y.Achour, T. Rekioua, "Tracking power photovoltaic system with sliding mode control strategy", *Terragreen13 International Conference, Energy Procedia* 36, pp.219-230, 2013
- [10] K. Punithaa, D. Devaraj, S. Sakthivel, "Development and analysis of adaptive fuzzy controllers for photovoltaic system under varying atmospheric and partial shading condition", *Applied Soft Computing* 13, pp.4320–4332, 2013
- [11] Anastasios I. Dounis, Panagiotis Kofinas, Constantine Alafodimos, Dimitrios Tseles, "Adaptive fuzzy gain scheduling PID controller for maximum power point tracking of photovoltaic system", *Renewable Energy* 60, pp.202-214,2013
- [12] Mustafa A. Al-Saffar, Esam H. Ismail, Ahmad J. Sabzali, "Family of ZC-ZVS converters with wide voltage range for renewable energy systems", *Renewable Energy* 56, pp.32-43, 2013
- [13] Bader N.Alajma, Khaled H.Ahmed, Stephen J.finnery, and Barry W.Williams, "Fuzzy-Logic-Control Approach of a Modified Hill-Climbing Method for Maximum Power Point in Microgrid Standalone Photovoltaic System", *IEEE Transaction on power electronics*, vol.26, no.4, pp.1022-1030, april 2011

- [14] Azadeh Safari and Saad Mekhilef, "Simulation and Hardware Implementation of Incremental Conductance MPPT with Direct Control Method Using Cuk Converter", *IEEE Transactions on Industrial Electronics*, vol. 58, no. 4, pp.1154-1161, april 2011
- [15] Fangrui Liu, Shanxu Duan, Fei Liu, Bangyin Liu, and Yong Kang, "A Variable Step Size INC MPPT Method for PV Systems", *IEEE Transactions on Industrial Electronics*, vol. 55, no. 7, pp.2622-2628, july 2008
- [16] Qiang Mei, Mingwei Shan, Liying Liu, and Josep M. Guerrero, "A Novel Improved Variable Step-Size Incremental-Resistance MPPT Method for PV Systems", *IEEE Transactions on Industrial Electronics*, vol. 58, no. 6, pp. 2427-2434, june 2011
- [17] R.Arulmurugan and N.Suthanthiravanitha, "Improved Fractional Order VSS Inc-Cond MPPT Algorithm for Photovoltaic Scheme", *International Journal of Photoenergy*, vol. 2014, Article ID 128327, 10 pages, 2014. (DOI:10.1155/2014/128327).
- [18] Trishan ESRAM, and Patrick L. Chapman, "Comparison of Photovoltaic Array Maximum Power Point Tracking Techniques", *IEEE Transactions on Energy Conversion*, VOL. 22, NO. 2, pp. 439-449, JUNE 2007
- [19] Arulmurugan, R.,Suthanthira Vanitha, N., "Intelligent Fuzzy MPPT Controller using Analysis of DC to DC Novel Buck Converter for Photovoltaic Energy System Applications", *Proceedings of the 2013 International Conference on Pattern Recognition, Informatics and Mobile Engineering*, February 21-22, pp. 225-231
- [20] M.H. Taghvaei, M.A.M.Radzi, S.M.Moosavain, Hashim Hizam, M.Hamiruce Marhaban, "A current and future study on non-isolated DC-DC converters for photovoltaic applications", *Renewable and Sustainable Energy Reviews* 17, pp.216-227, 2013